#312

Next-Generation Enzyme Replacement Strategies for Gaucher Disease

Sarlé P[1,2], Pradas Sarlé E[1,2], Castillo-Sánchez P[2], Arrúe-Gonzalo M[2], Tanco S[1], Carnicer-Caceres C[3], Castillo-Ribelles L[3], Artola M[4], Vicent MJ[5], Martinez-Vicente M[2], Lorenzo J[1]

[1]Protein Engineering and Nanomedicine group. Universitat Autònoma de Barcelona (UAB), Spain. [2]Neurodegenerative diseases group, Vall d'Hebron Research Institute (VHIR)-CIBERNED-UAB, Spain. [3]Biochemistry Service, Vall d'Hebron Hospital, Barcelona, Spain. [4]Department of Medical Biochemistry, Leiden Institute of Chemistry, Leiden University, Leiden, The Netherlands. [5]Polymer Therapeutics Lab. Centro de Investigación Príncipe Felipe (CIPF), Valencia, Spain

Next-Generation Enzyme Replacement Strategies for Gaucher Disease

Sarlé, P[1,2]; Pradas, E[1,2]; Castillo-Sánchez, P[2]; Arrúe-Gonzalo, M[2]; Tanco, S[1]; Carnicer-Caceres C[3], Castillo-Ribelles L[3]; Artola, M[4]; Vicent, MJ[5]; Martinez-Vicente, M[2]; Lorenzo, J[1]

1 Protein Engineering and Nanomedicine group. Universitat Autònoma de Barcelona (UAB), Spain. 2 Neurodegenerative diseases group, Vall d'Hebron Research Institute (VHIR)-CIBERNED-UAB, Spain. 3 Biochemistry Service, Vall d'Hebron Hospital, Barcelona, Spain. 4 Department of Medical Biochemistry, Leiden Institute of Chemistry, Leiden University, Leiden, The Netherlands. 5 Polymer Therapeutics Lab. Centro de Investigación Príncipe Felipe (CIPF), Valencia, Spain

Introduction

Enzyme replacement therapy (ERT) has revolutionized the management of patients with lysosomal storage disorders (LSDs) over the last few decades. Periodic intravenous administration of active GBA has proven effective in reversing most visceral manifestations of Gaucher Disease (GD). However, there are important drawbacks associated with ERT, such as GBA poor stability and inactivation in the bloodstream leading to high and frequent doses. To overcome these challenges, we have optimized the production and purification of different GBA glycoforms in a mammalian expression system obtaining two cost-effective GBA variants with catalytic properties comparable to an FDA approved one. To further improve ERT strategy our team has developed the NanoGBA, integrating a biodegradable peptidic based polymer that enhances protein stability, bioavailability, and targeted biodistribution.

Mammalian expression system scheme

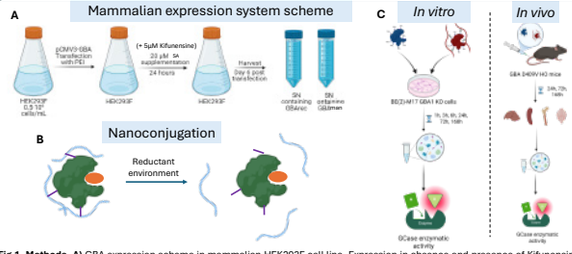

Fig 1. Methods. A) GBA expression scheme in mammalian HEK293F cell line. Expression in absence and presence of Kifunensine leads to GBArec and GBAman respectively. **B)** Graphic representation of NanoGBA technology. **C)** Graphic representation of GBA and NanoGBA treatments *in vitro* using BE(2)M17 GBA KO cells (left) and *in vivo* in GBA D409V homozygote mice (right).

GBA production optimization

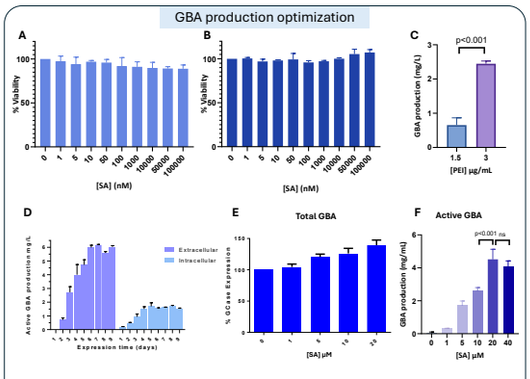

Fig 2. Optimization of GBA expression. A,B) Cytotoxic assay in HEK293F cells was performed at SA concentrations in a range between 1 and 10.000 nM, at 24 (A) and 72 hours (B). **C)** Quantity of transfection agent PEI was optimized assessing the levels of GBA produced. **D)** Active GBA found over time in the extracellular medium (dark) or intracellular (light) of HEK293F pCMV3GBA-transfected cells. **E,F)** Quantification of total (E) and active (F) GBA found in the extracellular media at day 6 post transfection under the presence of different amounts of the stabilizing agent (SA). All data is represented as the mean +/- SD. (standard deviation) of three independent biological replicates.

GBA characterization

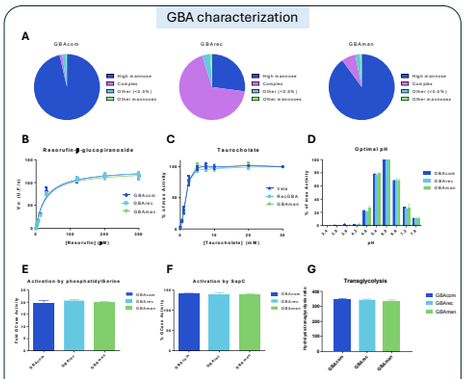

Fig 3. Characterization of two GBA glycoforms. A) Glycan composition determined by LC-MS/MS analysis of a commercial GBA (GBAcom) and our in-house GBA expressed in absence (GBArec) or presence (GBAman) of kifunensine. **B)** Kinetic profile of GBAs against the substrate Resorufin-β-glucopyranoside (B) and the activator sodium taurocholate (C). **D)** Optimal pH determination. GBAs were incubated in activity buffer at different pH values and their catalytical activity was assessed. **E,F)** GBA activation through natural activators. GBA activity was assessed in activity buffer in the presence of phosphatidylserine (E) or Saposin C (F). **G)** Determination of hydrolysis:transglicolysis activity ratio of GBAs after an activity assay in the presence of cholesterol as a glucose acceptor. Data is represented as the mean +/- SD. (standard deviation) of three independent replicates.

GBA therapeutic effect

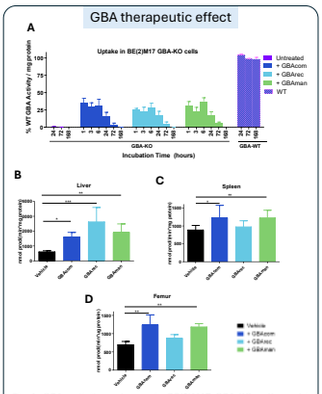

Fig 4. GBA activity restorage in BE(2)M17 GBA-KO cells and in GBA D409V HO mice. A) Quantification of GBA activity in cell lysates after GBA treatment up to 7 days. Data is represented as a percentage of GBA activity in BE(2)M17 wild type cells (WT). **B,C,D)** GCase activity recovery in liver (B), Spleen (C), and Femur (D) 24 hours after intravenous treatments of GBAs. Data is represented as the mean +/- SD ***P<0,001; **P<0,01, *P<0,05 after Welch ANOVA followed by Games-Howell's multiple comparison test.

NanoGBA Lysosomal GBA recovery *in vitro*

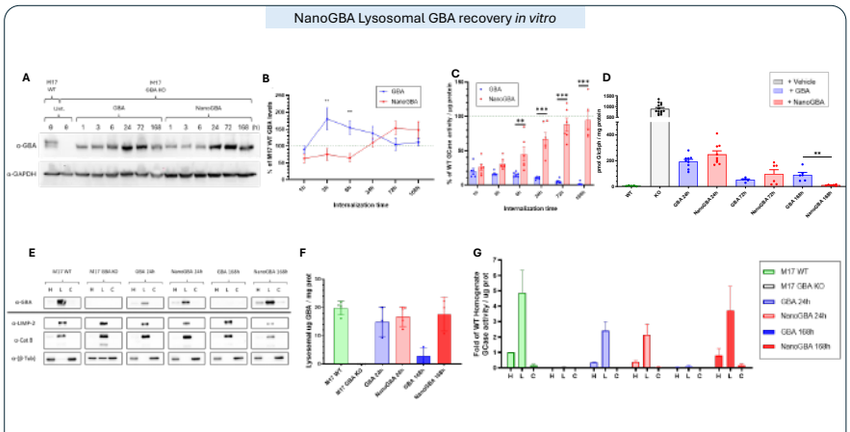

Fig 5. Comparative uptake of recombinant GBA and NanoGBA up to 7 days in BE(2)M17 GBA-KO cells. A) Immunodetection of GBA by western blot at different timepoints after NanoGBA or GBA treatment. **B)** Quantification of GBA protein after both treatment, endogenous GBA levels in BE(2)M17 WT cells is represented as a dash line. **C)** Quantification of GBA activity in cell lysates after both treatments, basal GBA activity in BE(2)M17 WT cells is represented as a dash line. **D)** Substrate levels after both treatments were quantified as HexSph (LysoGb1) by HPLC-MS/MS). **E)** Immunodetection of GBA and some organelle markers in the different fractions upon a subcellular fractionations of BE(2)M17 WT or KO GBA1 cells previously treated with either free GBA or NanoGBA (homogenate: H, lysosomal fraction: L and cytosol: C) **F)** Quantification of total GBA protein in the lysosomal fraction expressed as μg of GBA / mg of protein. **G)** GBA activity of each fraction represented as fold of the M17 WT GBA activity per μg of total protein at the homogenate fraction. Data is represented as the mean +/- SD of three independent replicates. ***P<0,001; **P<0,01 after one way ANOVA followed by Tukey's multiple comparisons test.

NanoGBA biodistribution *in vivo*

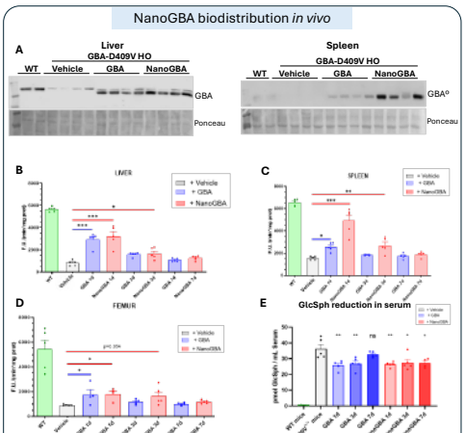

Fig 6. Biodistribution of GBA and NanoGBA after single-dose intravenous administration in GBA D409V HO mice. A) Immunodetection by western blot of GBA in liver (left) and spleen (right) 24 hours after intravenous administration of GBA or NanoGBA. **B,C,D)** GBA activity recovery in liver (B), Spleen (C), and Femur (D) 1, 3 or 7 days after intravenous treatments of GBA or NanoGBA. **E)** Comparative sphingolipid (GlcSph) analysis in serum at the indicated times. Data is represented as the mean +/- SD ***P<0,001; **P<0,01, *P<0,05 after Welch ANOVA followed by Games-Howell's multiple comparison test.

Conclusions

- GBA production can be optimized by enzyme stabilization during expression.
- GBA glycosylation modulates biodistribution *in vivo* without affecting its catalytical properties.
- Nanoconjugation enhances GBA stability and cellular uptake.
- *In vitro* NanoGBA treatment efficiently delivers exogenous GBA to lysosomes,
- *In vivo* intravenous NanoGBA administrations improves biodistribution in target tissues.

Contact us!

Pau Sarlé Vallés

pau.sarle@uab.cat

Personal LinkedIn

NanoERT LinkedIn

Presentado en el 22st Annual WORLDSymposium February 2-6, 2026 San Diego.

REFERENCIA:
Abstracts / Molecular Genetics and Metabolism 147 (2026) 109295.
doi:10.1016/j.ymgme.2025.109610

MAT-ES-2600293 v1 Marzo 2026

Los datos y análisis presentados en este póster fueron originalmente expuestos en el 22nd *Annual World Symposium* (2-6 febrero de 2026), cumpliendo con los estándares de presentación científica de dicho evento.